35th International Electric Vehicle Symposium and Exhibition (EVS35)
Oslo, Norway, June 11-15, 2022

Experimental study on half-cell impedance of lithium-ion battery considering various alternating current amplitudes

Ranjun Huang[1,2], Heze You[1,2], Guangxu Zhang[1,2], Siqi Chen[1,2], Bo Jiang[1,2], Jiangong Zhu[1,2], Xuezhe Wei[1,2], Haifeng Dai[1,2*]

[1] *Clean Energy Automotive Engineering Center, Tongji University, 4800 Caoan Road, Shanghai,201804, China*

[2] *School of Automotive Studies, Tongji University, 4800 Caoan Road, Shanghai,201804, China*

tongjidai@tongji.edu.cn

Summary

The magnitude of the battery impedance is affected by different alternating currents. At present, most researchers focus on the influence of alternating current (AC) frequency on impedance, but there is little research on that of AC amplitude. This paper aims to investigate the influence of various AC amplitudes at low and room temperatures (-10℃, 25℃) on the half-cell impedance of lithium-ion battery with different state of charge (SOC) based on a series of experiments. Finally, the internal mechanism of the effect of AC impedance on lithium-ion impedance will be revealed.

Keywords: EV, lithium-ion battery, impedance spectroscopy, electrode, internal resistance

1 Introduction

Due to the high heating efficiency and low energy consumption, the alternating current (AC) heating of lithium-ion batteries in a low-temperature environment has been widely studied. At present, when calculating the heat generation inside the battery, most researchers only consider the effects of AC frequency, temperature, and state of charge on battery impedance[1-6], ignoring the influence of AC amplitude on impedance. It may affect the accuracy of the battery thermal model, which in turn affects the development of heating strategies. In addition, studying the impedance at different AC amplitudes allows us to understand the mechanism of the electrode kinetics. And the more accurate battery dynamics model can be built. Although Zhu et al.[7,8] studied the relation between AC heating amplitude and battery impedance, it was from the perspective of the whole battery. Given the above deficiencies, this paper designs experiments to study the influence of AC heating amplitude on half-cell impedance under different SOC at room and low temperatures.

2 Experiments

2.1 Making half cells

The sample lithium-ion battery is a NCA battery with a nominal capacity of 1 Ah. The operating voltage range is 3V~4.2V. The half cells are CR2016 type coin cells. They have anode or cathode as the working electrode and metallic lithium as a counter electrode. The working electrodes are obtained from the sample battery with 14 mm diameter. The capacity is 3.69mAh, which can be obtained through theoretical arithmetic. The main process for making coin cells under argon atmosphere in a glove box is shown in Fig. 1.

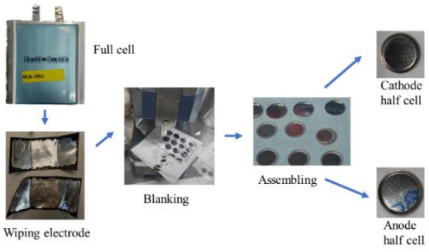

Figure1: The main process for making coin cells

2.2 The open circuit voltage (OCV) tests

To obtain the corresponding relationship of OCV among full cell and two half cells, the same rate charge and discharge (0.05C) are developed to assess the full cell's performance using MACCOR MC8, and the electrochemical workstation (Solartron SI 1287, 1255B) is used to measure the OCV of half cells. The temperature is kept at 25℃ by DONG&YE C7-340 Pro. Different from the full cell, the OCV of half cells can be measured by constant current charging and discharging at a small rate. In this paper, 70uA (0.02C) is chosen to avoid excessive polarization voltage. The cathode half cell's charging and discharging cut-off voltages are 4.3V and 2.8V respectively, and those of anode half cell are 2V and 0.01V.

2.3 Measurement of the electrochemical impedance spectroscope (EIS) with different current amplitudes

The EIS tests with different current amplitudes are conducted on the half cells at the specified SOC, i.e., 20%, 50%, 80%. The excitation frequency range is from 0.002Hz~1000kHz and the excitation current amplitudes are 0.01mA, 0.05mA, 0.1mA, 0.5mA, 1mA, 2 mA and 3 mA. In addition, it should be noted that the excitation current will be adaptively adjusted according to the OCV of half cells. And the measured half cell is placed in the thermal chamber at the specified temperature for more than 3 h to guarantee temperature equilibration before conducting tests. The experiences are carried out at -10℃ and the results at 25℃ are also investigated for comparison. The test bench is shown in Fig. 2.

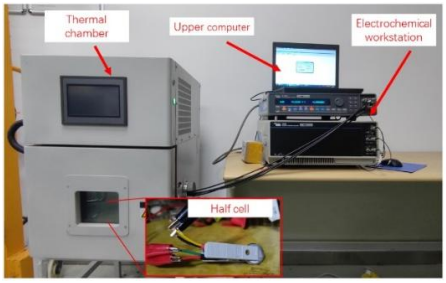

Figure2: The testbench for coin cells

3 Results and Discussion

3.1 The relation of OCV among full cell and half cells

In order to determine the corresponding relationship of voltage between the full cell and the half cell under different SOCs, it is necessary to reconstruct the full cell voltage by using the half cell voltage data. Referring to the work of Ge et al.,[9] the calculation formula can be expressed as

$$OCV(SOC) = U_c((x_{c,100\%} - x_{c,0\%})SOC + x_{c,0\%}) - U_a((x_{a,100\%} - x_{a,0\%})SOC + x_{a,0\%}) \quad (1)$$

where x means the stoichiometric coefficient "x" in Li_xC_6 and $Li_xNi_aCo_bAl_cO_2$ (a + b + c = 1). The $x_{a,100\%}$ and $x_{a,0\%}$ are stoichiometric coefficients in anode, $x_{c,100\%}$ and $x_{c,0\%}$ are stoichiometric coefficients in cathode at the 100% and 0% SOC of the full cell. OCV(SOC) represents the relationship between full cell OCV and SOC. $U_c(x)$ and $U_a(x)$ represent the relationship between cathode and anode potentials and stoichiometric coefficient, respectively. And then the genetic algorithm is used to identify $x_{a,100\%}$, $x_{a,0\%}$, $x_{c,100\%}$ and $x_{c,0\%}$. The result is shown in Fig. 3.

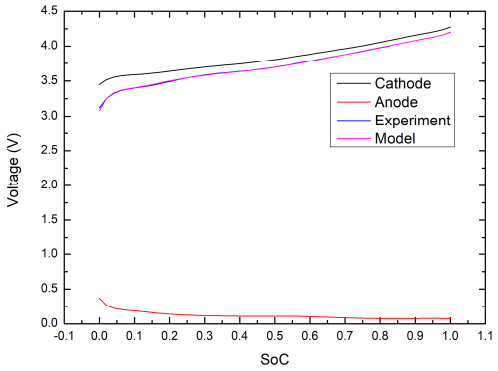

Figure3: The voltages between the full cell and the half cell under different SOCs

In this paper, the impedances of anode and cathode under different magnitudes are investigated at full cell SOC of 0.2, 0.5 and 0.8. The corresponding anode and cathode voltages are shown in Table 1. However, due to the influence of the experimental progress, the cathode experiment is still in progress. Therefore, the following will mainly analyze the experimental results of anode half cell.

Table1: The Anode potentials of anode and cathode under different SOCs

Full cell SOC	0.2	0.5	0.8
Anode potential	0.137V	0.109V	0.076V
Cathode potential	3.638V	3.805V	4.054V

3.2 Anode impedance under different alternating current amplitudes

Fig. 4 and Fig. 5 show the results of the experiments at 25℃ and -10℃. Considering that the small AC amplitude test at high frequency is easily interfered with by measurement noise, such as some measurement results of 0.01mA at high frequency (>10^5Hz), these unreasonable points have been deleted from the figures. In the two figures, a, d and g represent the impedance spectroscopy with different AC amplitudes; b, e and h represent the relationship between the real part and frequency; c, f and i represent the relationship between phase and frequency. The three graphs in the same row, such as a, b and c; d, e and f; g, h and i, represent the results measured at 0.137V, 0.109V and 0.076V, respectively. To understand the variation of impedance spectra clearly, the frequency variation of impedance spectroscopy at different AC amplitudes is shown in Fig. 6.

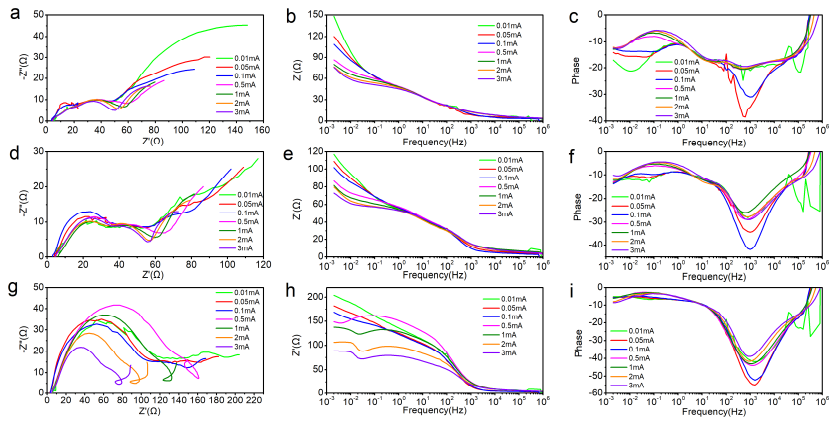

Figure4: EIS, the real parts and phases of anode half cell measured at 25 ℃ and different AC amplitudes: a,b,c 0.137V; d,e,f 0.109V; g,h,i 0.076V.

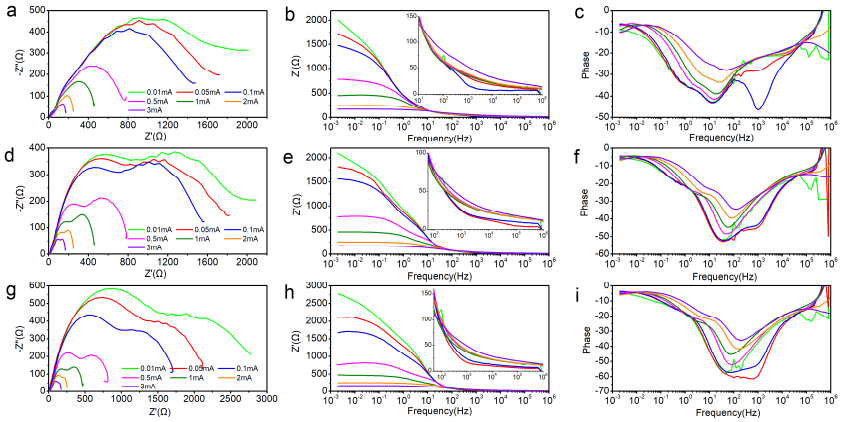

Figure5: EIS, the real parts and phases of anode half cell measured at -10 ℃ and different AC amplitudes: a,b,c 0.137V; d,e,f 0.109V; g,h,i 0.076V.

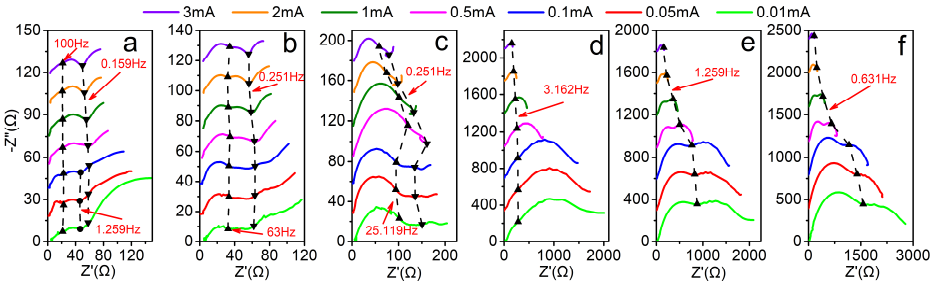

Figure6: Frequency variation of impedance spectra at different AC amplitudes: a,b,c 25℃; d,e,f -10℃; a,d 0.137V; b,e 0.109V; c,f 0.076V.

At room temperature, it can be seen from Fig. 4 that the arc in impedance spectroscopy gradually becomes larger as the anode Anode potential decreases. And the law also exists in Fig. 5. This phenomenon may be due to the change of physical and chemical properties in graphite after the occurrence of lithium intercalation. And then, different AC amplitudes have different effects on impedance spectroscopy, which can be divided into two categories: the current amplitudes of 0.01mA, 0.05mA and 0.1mA and the current amplitudes of 0.5mA, 1mA, 2mA and 3mA. The two categories are respectively denoted as (I) and (II). From the real parts of impedance and phases at different frequencies in Fig. 4b, c, e and f, we can see that there are obvious differences between (I) and (II). At 0.137V and 0.109V, the high-frequency arcs of (I) are larger. The high-frequency arcs of (II) basically coincide. However, the medium-frequency arcs are different from high-frequency arcs. The medium-frequency arcs of (I) basically coincide. And the medium-frequency arcs of (II) gradually shrink with the increase of AC amplitude. For the low-frequency range, we can see from Fig. 4 b and e that the real parts decrease with the increase of AC amplitude. In addition, Fig. 6 also shows that the frequency changes of (I) and (II)'s impedance spectroscopy are different with the increase of the AC amplitude at 25℃. The frequencies marked in Fig. 6 are all at the junctions of different impedance arcs. For 0.137V, the minimum frequencies of the medium-frequency arcs in (I) and (II) are different: (I) is 1.259Hz, (II) is 0.159Hz. In addition, the real parts of the high-frequency and the medium-frequency impedance in (I) hardly change with different AC amplitudes. However, it can be seen that the real parts of the medium-frequency impedance in (II) decrease with the increase of AC amplitude. This phenomenon also occurs at 0.109V and 0.076V. And the difference between (I) and (II) is more obvious at 0.076V. From Fig. 4 g and h, we can see that not only the medium-frequency arcs shrink, but the high-frequency arcs also shrink. This indicates that (I) and (II) have different effects on the anode kinetic process at 25 °C, and are more pronounced at the higher lithiation state. Although the (I) and (II) have different effects on impedance, there is a critical frequency x (1Hz<x<10Hz) that separates the real parts of impedance into two regions, one of which is the amplitude-independent region at high frequencies and the other is the amplitude-dependent region at medium and low frequencies. In addition, because the high-frequency arcs also shrink, the frequency x becomes larger at 0.076V. It should be noted that the "amplitude-independent region" does mean that the real parts of impedance and AC amplitude are

completely irrelevant, but the real parts of impedance at high frequencies are much less affected by the AC amplitude than those at medium and low frequencies. This experimental phenomenon is the same as that of Zhu et al.[7] for full cell.

At low temperature, we can see from Fig. 5 that the impedance arcs shrink more severely with the increase of AC amplitude. And the voltage of anode does not seem to affect the relationship between the impedance arc and the AC amplitude. As can be seen in Fig. 5 b, e and h, the frequency at which the impedance arc begins to shrink is between 10Hz and 100Hz. And the frequency is the frequency *x* above. When the frequency is bigger than *x*, although the real parts of the impedance are different under different AC amplitudes, the difference is small compared with the low-frequency range (<*x*). And at low temperature, the phase difference of impedance spectroscopy at different AC amplitudes is larger than that at room temperature. Another interesting finding is that the intersection frequencies of different arcs at low temperature vary with the AC amplitude. As shown in Fig. 6 d, e and f, the frequency dotted lines in the figure are selected as the intersection frequencies of different arcs when the AC amplitude is 0.01mA. It can be seen that the frequency gradually becomes the frequency on a certain arc as the AC amplitude increases.

3.3 Discussion

The main phenomenon of the above experimental results is that when the frequency is bigger than a certain frequency x (1Hz<x<100Hz), the impedance arc will shrink with the increase of the AC amplitude. The experimental results are in good agreement at low temperature. However, the phenomenon is obvious only when the AC amplitude is bigger than a certain value 0.5mV at room temperature. For influencing factors, temperature and SOC are considered first. Although the temperature sensor is not used to measure the temperature of the coin cell, the temperature rise of the coin cell can be ignored because of the strong convection of the thermal chamber. In addition, the SOC change is approximately ±1.13% at the maximum AC amplitude (3mA) and 0.01Hz. It shows that the influence of SOC can be ignored.

Through full-cell experiments, Zhu et al.[7] showed that the charge-transfer process affects the shrinkage of medium-frequency impedance arc, and used the Butler-Volmer equation to fit the relationship between different AC amplitudes and the charge-transfer impedance under low-temperature conditions. However, according to the study by Koleti et al.[10], lithium planting can reduce the impedance, which leads to the shrinkage of medium-frequency impedance arc. Due to the increased internal resistance of the battery at low temperature, lithium planting is likely to occur when the AC amplitude is large. Therefore, to verify the above conjecture, another experiment is carried out. This experiment is carried out at another electrochemical workstation (Solartron Analytical 1400A,1470E) at room temperature, which can collect the current and voltage signals during the EIS test. And when the anode potential is 0.128V, the voltage responses of anode half cell with different AC amplitudes are shown in Fig. 7. However, it only acquires the data of the first 500s

because of the memory limit. For 1mA, we can see that the anode potential begins to appear less than 0V when the frequency is about 4Hz. According to the study of Waldmann et al.[11], lithium planting will occur when the potential of graphite is below 0V vs. Li/Li^+. As can be seen from Fig. 4, the difference between the impedance arcs of AC amplitude 1mA and 0.5mA begins to appear at a certain frequency between 1Hz and 10Hz. To some extent, it proves that lithium planting leads to the shrinkage of medium-frequency impedance arc. In addition, at low temperature, the increased internal resistance of lithium-ion battery increases the probability of lithium deposition in the anode. Therefore, it can be seen from Fig. 5 that the shrinkage of the impedance arc is more serious. This makes us realize that when studying the AC heating of lithium-ion battery, the effect of AC amplitude on the battery impedance needs to be considered.

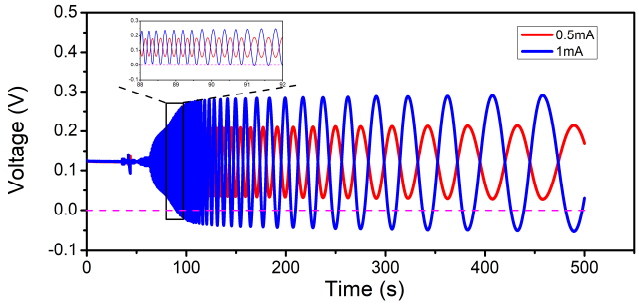

Figure7: Voltage responses of anode half cell with different AC amplitudes

4 Conclusions

This paper demonstrates anode half-cell impedance with different AC amplitudes at room and low temperatures. Results led to three key findings. Firstly, the impedance arc will shrink with the increase of the AC amplitude at low temperature. However, the phenomenon is obvious only when the AC amplitude is bigger than a certain value 0.5mV at room temperature. Secondly, the intersection frequencies of different impedance arcs at low temperature vary with the AC amplitude. But they are nearly unchanged at room temperature. Lastly, the shrinkage of anode impedance arc is related to lithium plating, especially at low temperature.

Acknowledgments

This work is financially supported by the National Natural Science Foundation of China (NSFC, Grant number U20A20310).

References

[1] Zhang J., Ge H., Li Z., et al., Internal heating of lithium-ion batteries using alternating current based on the heat generation model in frequency domain. Journal of Power Sources, 2015.273: 1030-1037.

[2] Li J., Fang L., Shi W., et al., Layered thermal model with sinusoidal alternate current for cylindrical lithium-ion battery at low temperature. Energy, 2018.148:247-257.

[3] Wu X., Cui Z., Chen E., et al., Capacity degradation minimization oriented optimization for the pulse preheating of lithium-ion batteries under low temperature. Journal of Energy Storage, 2020. 31.

[4] Zhang L., Fan W., Wang Z., et al., Battery heating for lithium-ion batteries based on multi-stage alternative currents. Journal of Energy Storage, 2020. 32.

[5] Guo S., Xiong R., Wang K., et al., A novel echelon internal heating strategy of cold batteries for all-climate electric vehicles application. Applied Energy, 2018. 219:256-263.

[6] Ruan H., Jiang J., Sun B., et al., A rapid low-temperature internal heating strategy with optimal frequency based on constant polarization voltage for lithium-ion batteries. Applied Energy, 2016. 177: 771-782.

[7] Zhu J., Sun Z., Wei X., et al., Studies on the medium-frequency impedance arc for Lithium-ion batteries considering various alternating current amplitudes. Journal of Applied Electrochemistry, 2015.46(2):157-167.

[8] Zhu J., Sun Z., Wei X., et al., An alternating current heating method for lithium-ion batteries from subzero temperatures. International Journal of Energy Research, 2016.40(13):1869-1883.

[9] Ge H., Aoki T., Ikeda N., et al., Investigating Lithium Plating in Lithium-Ion Batteries at Low Temperatures Using Electrochemical Model with NMR Assisted Parameterization. Journal of The Electrochemical Society, 2017.164(6): A1050-A1060.

[10] Koleti U.R., Dinh T.Q., and Marco J., A new on-line method for lithium plating detection in lithium-ion batteries. Journal of Power Sources, 2020. 451.

[11] Waldmann T, Hogg B I, Wohlfahrt-Mehrens M. Li plating as unwanted side reaction in commercial Li-ion cells – A review. Journal of Power Sources, 2018, 384(4): 107-124.

Authors

Ranjun Huang received the B.S. degree in automotive engineering from Wuhan University of Technology, Wuhan, China, in 2017, and the M.S. degree in mechanical engineering from Hunan University, Changsha, China, in 2020. He is currently pursuing the Ph.D. degree with the School of Automotive Studies, Tongji University, Shanghai, China.

His research interests focus on batteries, including performance degradation, heating and charging at low temperature.

Heze You received the B.S. degree in automotive engineering from Hunan University, Changsha, China, in 2017. He is currently working toward the Ph.D. degree with the School of Automotive Studies, Tongji University, Shanghai, China.

His research interests include battery non-linear aging mechanism, non-linear electrochemical modeling, and non-linear aging prediction and evaluation.

Guangxu Zhang is currently a Ph.D. candidate in the School of Automotive Studies, Tongji University. He received his B.S. degrees from Hunan University in 2018. He has co-authored more than 10 research papers published in refereed journals and has applied for more than 20 patents.

His current research is focusing on the thermal safety and degradation mechanism of lithium-ion batteries during the whole life cycle.

Siqi Chen is currently pursuing the Ph.D. degree with the School of Automotive Studies, Tongji University, Shanghai, China.

His research interests include battery safety, advanced battery thermal management technologies and multi-objective optimization design.

Bo Jiang received the B.S. degree in automotive engineering from Harbin Institute of Technology, Weihai, China, in 2015, and the Ph.D. degree in automotive engineering from Tongji University, Shanghai, China, in 2021.

He is now a Postdoc with the School of Automotive Studies, Tongji University. His research interests include battery modeling and advanced state estimation technologies in the battery management system.

Dr. Jiangong Zhu is an Associate Professor in the School of Automotive Studies at Tongji University, China. He received the Ph.D. degree in automotive engineering at Tongji University. He was a Post-Doctoral Researcher at the Institute for Applied Materials at the Karlsruhe Institute of Technology (KIT) in Germany. He is a “Humboldtians” Fellow from the support of Humboldt Foundation and a DAAD (Deutscher Akademischer Austausch Dienst) fellow.

His research interests include electric vehicles, lithium-ion batteries, battery lifetime and safety management, state estimation, and battery modeling. His current research focus is on applying the ex-situ (post-mortem analysis) and in-situ methods (e.g., impedance, neutron powder diffraction) to investigate the battery degradation, and inventing new science methods (e.g., machine learning and optimization) to prognose the battery state of health and manage the power battery lifespan. His research has been sponsored by National Natural Science Foundation of China and awarded “Shanghai Overseas High-Level Talent Recruitment Program” in 2021.

Xuezhe Wei received the B.S. and M.S. degrees in electrical engineering and the Ph.D. degree in automotive engineering from Tongji University, Shanghai, China, in 1994, 1997, and 2005 respectively.

He is currently a Professor with the School of Automotive Studies, Tongji University. His research interests include battery system management, fuel cell system control, as well as electrical power conversion for electric vehicles.

Haifeng Dai received the B.S. and M.S. degrees in mechanical engineering and the Ph.D. degree in automotive engineering from Tongji University, Shanghai, China, in 2003, 2005, and 2008 respectively.

He is currently a Professor with the School of Automotive Studies, Tongji University. His research interests include battery system management, fuel cell system control, as well as electrical power conversion for electric vehicles.